



**HAL**  
open science

## Wiener interpolation filter for phase noise estimation in sub-THz transmission

Yaya Bello, Jean-Baptiste Dore, David Demmer

► **To cite this version:**

Yaya Bello, Jean-Baptiste Dore, David Demmer. Wiener interpolation filter for phase noise estimation in sub-THz transmission. IEEE VTC-Spring - 2023 IEEE 97th Vehicular Technology Conference, Jun 2023, Florence, Italy. , 2023, pp.1-5, 2023, 2023 IEEE 97th Vehicular Technology Conference (VTC2023-Spring). 10.1109/VTC2023-Spring57618.2023.10200443 . cea-04371974

**HAL Id: cea-04371974**

**<https://cea.hal.science/cea-04371974>**

Submitted on 4 Jan 2024

**HAL** is a multi-disciplinary open access archive for the deposit and dissemination of scientific research documents, whether they are published or not. The documents may come from teaching and research institutions in France or abroad, or from public or private research centers.

L'archive ouverte pluridisciplinaire **HAL**, est destinée au dépôt et à la diffusion de documents scientifiques de niveau recherche, publiés ou non, émanant des établissements d'enseignement et de recherche français ou étrangers, des laboratoires publics ou privés.

# Wiener Interpolation Filter for Phase Noise Estimation in sub-THz Transmission

Yaya Bello, Jean-Baptiste Doré, David Demmer  
CEA-Leti, Univ. Grenoble Alpes, F-38000 Grenoble, France  
{yaya.bello, jean-baptiste.dore, david.demmer}@cea.fr

**Abstract**—High frequency transmissions above 90 GHz, as planned for the future generation of communication technology called 6G, have to deal with oscillator-induced phase noise. This phase noise deteriorates the system performance and then, signal processing techniques are mandatory to counteract its effects. In this paper, we describe and analyze a phase noise estimation algorithm based on an Wiener interpolation filter. The proposed technique is waveform agnostic and can be applied either to 5G-NR multicarrier waveforms such as orthogonal frequency division multiplexing (OFDM) and discrete Fourier transform spread OFDM (DFT-s-OFDM), or to single carrier systems. In this study, we highlight the feasibility of this algorithm in practical scenarios by providing both a theoretical analysis and a performance evaluation.

**Index Terms**—Single-Carrier, OFDM, DFT-s-OFDM, 5G-NR PTRS, 6G.

## I. INTRODUCTION

The availability of large bandwidths in sub-THz bands [1] allows to consider these bands as a key solution for future wireless communications [2]. They will permit the increase of the communication system capacity, notably the throughput. However, transmitting in sub-THz bands has some hardware constraints, including phase noise (PN) generated by the oscillators. Consequently, PN compensation is required to enhance the system performance. In this paper, we show the feasibility of implementing the PN compensation algorithm named interpolation filter (IF) in a real scenario.

Different PN estimation techniques are presented in the state-of-the-art. Most of them are designed for orthogonal frequency division multiplexing (OFDM) systems, such as ICI cancellation [3], [4]. In discrete Fourier transform-spread-OFDM (DFT-s-OFDM) systems, some PN estimation algorithms are described in [5] such as common phase error estimation (CPEE), linear interpolation (LI), discrete cosine transform (DCT), Kalman filter. CPEE and LI algorithms are considered in this work because of their low complexity implementation.

Exploiting the correlated nature of the PN is a promising approach already addressed in a recent literature. The authors in [6] present a novel technique applied to OFDM systems, which exploits the propagation channel estimation. Another algorithm, which exploits an *a priori* knowledge of stochastic properties of PN, *i.e.* its power spectral density (PSD), is introduced in [7]. Performance comparison considering a DFT-s-OFDM system is given in [7], by considering the IF algorithm and other estimation algorithms. The use of the IF leads to a good estimation of PN and therefore, the improvement of the system performance after PN compensation is highlighted.

In addition, the IF provides better performance when low pilot density is considered, which is important to increase the spectral efficiency. In this work, we show the possibility of implementing the IF algorithm for different communication systems.

The main technical contributions of this work are as follows:

- Theoretical expression of the PN cross-correlation matrix assuming the knowledge of its power spectral density (PSD).
- Theoretical expression of the mean square error (MSE) between the estimated PN and the generated one for a single-carrier system. We present a comparison between the theoretical MSE and the Monte-Carlo one.
- Uncoded bit error rate (BER) performance considering the IF algorithm and a single-carrier system. We use the theoretical cross-correlation matrix of the PN and the Monte-carlo one.
- Coded transport block error rate (TBLER) performance using 5G new radio (5G-NR) multicarrier waveforms and extended numerologies as in [8].

## Notations

In what follows, underlined lower boldface letters,  $\underline{\mathbf{a}}$ , indicate column vectors, with  $a_k$  denoting the  $k^{th}$  element of the column vector. The term  $E[\cdot]$  denotes the expectation operator. The term  $\mathbf{A}^{-1}$  represents the inverse of the matrix  $\mathbf{A}$ . The symbols  $|\cdot|$ ,  $\arg(\cdot)$ ,  $(\cdot)^T$ ,  $(\cdot)^*$ ,  $(\cdot)^H$ ,  $\Re\{\cdot\}$  and  $\Im\{\cdot\}$  respectively denote the magnitude value, the phase value, the transpose, the conjugate, the transpose-conjugate, the real part and the imaginary part. The matrix  $\mathbf{A}^\dagger$  which is defined as  $\mathbf{A}^\dagger = (\mathbf{A}^H \mathbf{A})^{-1} \mathbf{A}^H$  denotes the Moore-Penrose pseudo-inverse of matrix  $\mathbf{A}$ . Underlined boldface numbers  $\underline{\mathbf{N}}_X$  indicate column vectors of size  $X$ , and contain the number  $\mathbf{N}$  in all rows. Boldface numbers  $\mathbf{N}_X$  indicate matrices of size  $X \times X$  that fully contain the number  $\mathbf{N}$ . The operator  $\odot$  represents the Hadamard product.

## II. INTERPOLATION FILTER ALGORITHM

### A. System Model

Sparse channels are expected in sub-THz band transmission. The authors in [9] show that the use of high gain and directional antennas for RF transmission, ensure the most energy contribution of the line-of-sight (LoS) path. Consequently, NLoS paths are neglected and a LoS propagation frequency flat channel is considered in this work. We assume a coherent system with the presence of PN and a receiver synchronized in time and frequency. The PN model considered in this work

is the 3GPP PN model, where the PSD of the PN is given for both transmitter and receiver [10].

The proposed algorithm is a linear time-invariant filter used to estimate a PN random process of an observed noisy signal, assuming known stationary signal and PN spectra, as well as additive noise.

### B. Single-Carrier

The discrete-time received signal through an AWGN channel in the presence of PN, at the  $k^{\text{th}}$  sample is expressed as follows:

$$r_k = s_k e^{j\phi_k} + n_k, \quad (1)$$

where  $s_k$  and  $\phi_k$  respectively represent the transmitted signal and the discrete-time PN generated by the oscillators. The term  $n_k \sim \mathcal{CN}(0, \sigma_n^2)$  represents the thermal noise and  $\sigma_n^2$  its power. To apply the IF algorithm in single carrier system, we need to filter the received signal per block (that can be overlap). Let consider that we transmit a frame of  $N_p$  samples. We will compute the PN estimation per block of size  $N_a$  so that  $N_p = N_a \cdot N_b$ , where  $N_b$  represents the number of blocks. From (1) we have:

$$\mathbf{r}[m] = \mathbf{s}[m] \odot e^{j\phi[m]} + \mathbf{n}[m], \quad m = [0, N_b - 1]. \quad (2)$$

Assuming that the pilot symbols are inserted, let define  $\mathbf{a}_p$  as the vector that contains all the  $\{a_i\}_{i \in \chi_p}$  values such that:

$$a_i = \frac{r_i s_i^*}{|s_i|^2}, \quad \forall i \in \chi_p \quad (3)$$

where  $\chi_p$  represents the set that contains all the indexes where pilots are inserted. The terms  $r_i$  and  $s_i$  are respectively the received and inserted pilot symbols. Considering a single-carrier system, we obtain:

$$a_i = e^{j\phi_i} + \frac{n_i s_i^*}{|s_i|^2}, \quad \forall i \in \chi_p \quad (4)$$

Then, from (2) we have:

$$\mathbf{a}_p[m] = e^{j\phi_p[m]} + \mathbf{n}_p[m] \odot \mathbf{s}_p[m], \quad m = [0, N_b - 1] \quad (5)$$

where  $e^{j\phi_p}$  is the vector that contains all the  $\{e^{j\phi_i}\}_{i \in \chi_p}$  values and  $\mathbf{n}_p$  the one that contains  $\{n_i\}_{i \in \chi_p}$ . The vector  $\mathbf{s}_p$  contains all the  $\{\frac{s_i^*}{|s_i|^2}\}_{i \in \chi_p}$ . We can rewrite (5) as follows:

$$\mathbf{a}_p[m] = \mathbf{G}_p e^{j\phi[m]} + \mathbf{G}_p \mathbf{n}[m] \odot \mathbf{s}_p[m], \quad m = [0, N_b - 1] \quad (6)$$

where  $\mathbf{G}_p$  represents the pilot sampling matrix. Let us denote  $\mathbf{R}_{e^{j\phi}} = E[e^{j\phi} \cdot e^{j\phi H}]$  and  $\mathbf{R}_n = E[\mathbf{n} \cdot \mathbf{n}^H]$  as the covariance matrix respectively of  $e^{j\phi}$  and  $\mathbf{n}$ . The interpolation matrix  $\mathbf{Z}$  is derived as :

$$\min_{\mathbf{Z}} E[\|\mathbf{Z}\mathbf{a}_p - e^{j\phi}\|^2], \quad (7)$$

and is expressed as follows [7]:

$$\mathbf{Z} = \mathbf{R}_{e^{j\phi}}^H \mathbf{G}_p^H \mathbf{B}^\dagger, \quad (8)$$

where  $\mathbf{B} = \mathbf{C} + \mathbf{D}$  such that:

$$\begin{cases} \mathbf{C} = \mathbf{G}_p \mathbf{R}_{e^{j\phi}}^H \mathbf{G}_p^H, \\ \mathbf{D} = \left( \mathbf{G}_p \mathbf{R}_n^H \mathbf{G}_p^H \right) \odot \left( \mathbf{s}_p \mathbf{s}_p^H \right). \end{cases} \quad (9)$$

The expression of the estimated PN is obtained as follows:

$$\hat{\phi}[m] = \arg(\mathbf{Z} \cdot \mathbf{a}_p[m]), \quad (10)$$

and therefore from (2) the expression of the received samples after PN compensation is:

$$\hat{\mathbf{s}}[m] = \mathbf{r}[m] \odot e^{-j\hat{\phi}[m]}. \quad (11)$$

The estimation of the PN samples is obtained through the estimation of the exponential vector  $e^{j\phi}$  by using its cross-correlation matrix.

A second approach consists in using the cross-correlation matrix of the PN for the filter derivation, *i.e.*  $\mathbf{R}_\phi = E[\phi \cdot \phi^H]$ . Under the high signal-to-noise ratio (HSNR) approximation [11], the expression in (4) becomes:

$$a_i = e^{j\phi_i} \left( 1 + \frac{n'_i s_i^*}{|s_i|^2} \right), \quad \forall i \in \chi_p \quad (12)$$

where  $n'_i = n_i e^{-j\phi_i}$ . Then, from (12) we have:

$$\begin{aligned} \arg(a_i) &= \phi_i + \arctan\left(\frac{\Im\{n'_i s_i^*\}}{|s_i|^2 + \Re\{n'_i s_i^*\}}\right) \\ &\simeq \phi_i + \frac{\Im\{n'_i s_i^*\}}{|s_i|^2} \\ &\simeq \phi_i + \frac{\Im\{n''_i\}}{|s_i|}, \end{aligned} \quad (13)$$

where  $n''_i = n'_i e^{-js_{i\theta}}$  with  $s_{i\theta} = \arg(s_i)$ . In that case, the expressions in (5) and (6) become:

$$\begin{cases} \mathbf{a}_p^\theta[m] = \phi_p[m] + \mathbf{n}'_p[m] \odot \mathbf{s}_p[m], \\ \mathbf{a}_p^\theta[m] = \mathbf{G}_p \phi[m] + \mathbf{G}_p \mathbf{n}'[m] \odot \mathbf{s}_p[m], \end{cases} \quad (14)$$

where the vectors  $\mathbf{a}_p^\theta$  and  $\phi_p[m]$  respectively contain all the  $\{\arg(a_i)\}_{i \in \chi_p}$  and  $\{\phi_i\}_{i \in \chi_p}$ . The vectors  $\mathbf{n}'_p[m]$  and  $\mathbf{s}_p[m]$  respectively contain  $\{\Im\{n''_i\}\}_{i \in \chi_p}$  and  $\{\frac{1}{|s_i|}\}_{i \in \chi_p}$ .

So, let define  $\mathbf{R}_{\mathbf{n}'} = E[\mathbf{n}' \cdot \mathbf{n}'^H]$  as the cross-correlation matrix of  $\mathbf{n}'$ . Assuming that the thermal noise is circularly symmetric, we have:

$$E[\mathbf{n}'] = \mathbf{0}_{N_a} \quad \text{and} \quad \mathbf{R}_{\mathbf{n}'} = \frac{\mathbf{R}_n}{2}. \quad (15)$$

Therefore, the expression of the IF assuming the HSNR approximation is:

$$\mathbf{W} = \mathbf{R}_{\phi}^H \mathbf{G}_p^H \mathbf{B}^\dagger, \quad (16)$$

where  $\mathbf{B} = \mathbf{C} + \mathbf{D}$  such that:

$$\begin{cases} \mathbf{C} = \mathbf{G}_p \mathbf{R}_{\phi}^H \mathbf{G}_p^H, \\ \mathbf{D} = \left( \mathbf{G}_p \mathbf{R}_{\mathbf{n}'}^H \mathbf{G}_p^H \right) \odot \left( \mathbf{s}_p \mathbf{s}_p^H \right). \end{cases} \quad (17)$$

The estimated PN vector is expressed as follows:

$$\hat{\phi}[m] = \mathbf{W} \cdot \mathbf{a}_p^\theta[m], \quad \forall m = [0, N_b - 1] \quad (18)$$

and we recover the expression of the transmitted signal after PN compensation by computing the expression in (11). The HSNR approximation allows to directly estimate the PN by

using the cross-correlation matrix of the PN, rather than the one of the complex exponential of the PN. The size of interpolation matrices  $\mathbf{Z}$  and  $\mathbf{W}$  is  $N_a \times K$ , with  $N_a$  and  $K$  respectively are the number of samples and inserted pilots on each block.

### C. Multicarrier Waveforms: OFDM and DFT-s-OFDM

With multicarrier waveforms, the expression of the received signal impacted by PN is different than the single-carrier case. Indeed, the presence of PN causes a common phase error (CPE) and intercarrier interference (ICI) in the case of OFDM systems [3]. In DFT-s-OFDM systems, the PN induces the subcarrier phase error (SPE) and ICI [12]. As a consequence, we need to adapt the interpolation matrices to include the ICI terms. The expression of the interpolation matrix  $\mathbf{Z}$  can be written as follows [7]:

$$\mathbf{Z} = \mathbf{R}^H \mathbf{G}_p^H \mathbf{T}^\dagger, \quad (19)$$

where  $\mathbf{T} = \mathbf{M} + \mathbf{I} + \mathbf{N}$  such that:

$$\begin{cases} \mathbf{M} = \mathbf{G}_p \mathbf{R}^H \mathbf{G}_p^H, \\ \mathbf{I} = \left( \mathbf{G}_p \mathbf{R}_I^H \mathbf{G}_p^H \right) \odot \left( \mathbf{s}_p \mathbf{s}_p^H \right), \\ \mathbf{N} = \left( \mathbf{G}_p \mathbf{R}_n^H \mathbf{G}_p^H \right) \odot \left( \mathbf{s}_p \mathbf{s}_p^H \right). \end{cases} \quad (20)$$

The size of the matrix  $\mathbf{Z}$  is  $N_s \times K$  where  $K$  is the number of inserted pilots on each DFT-s-OFDM and OFDM symbols. The term  $N_s$  is the size of the spreading DFT in DFT-s-OFDM system and the activated subcarriers in OFDM system. The matrices  $\mathbf{R}_I$  and  $\mathbf{R}_n$  are respectively the cross-correlation matrix of the ICI and thermal noise. The term  $\mathbf{R}$  represents the cross-correlation matrix of the phase noise after Fourier transform. It is expressed as follows:

$$\begin{cases} \mathbf{R} = E \left[ \underline{\mathbf{C}}_{PE} \cdot \underline{\mathbf{C}}_{PE}^H \right] & \text{for OFDM systems,} \\ \mathbf{R} = E \left[ e^{j\phi'} \cdot e^{j\phi'^H} \right] & \text{for DFT-s-OFDM systems [7].} \end{cases} \quad (21)$$

The vector  $\underline{\mathbf{C}}_{PE}$  is the vector which contains the CPE in all rows. The term  $e^{j\phi'}$  represents the exponential of the new PN vector  $\phi'$  obtained after fast Fourier transformations. The expression of the estimated PN is obtained as follows:

$$\hat{\phi}' = \hat{\phi}'_{CPE} = \arg \left( \mathbf{Z} \cdot \underline{\mathbf{a}}_p \right), \quad (22)$$

where  $\underline{\mathbf{a}}_p$  contains all the  $\{a_i\}_{i \in \chi_p}$  values defined in (4), with respect to the multicarrier waveform system used. The expressions of the received OFDM and DFT-s-OFDM symbol after the PN compensation are:

$$\begin{cases} \hat{\mathbf{S}}[m] = \mathbf{R}[m] \odot e^{-j\hat{\phi}'_{CPE}[m]} & \text{for OFDM systems,} \\ \hat{\mathbf{s}}[m] = \mathbf{r}[m] \odot e^{-j\hat{\phi}'[m]} & \text{for DFT-s-OFDM systems,} \end{cases} \quad (23)$$

where  $\hat{\mathbf{S}}[m]$  and  $\mathbf{R}[m]$  are respectively the  $m^{\text{th}}$  transmitted and received OFDM symbol in the frequency domain. The terms  $\hat{\mathbf{s}}[m]$  and  $\mathbf{r}[m]$  are respectively the  $m^{\text{th}}$  transmitted and received DFT-s-OFDM symbol in the discrete-time domain.

**Remark:** For OFDM systems, the cross-correlation matrix in (21) is a fully CPE matrix because

$$\mathbf{R} = E \left[ \underline{\mathbf{C}}_{PE} \cdot \underline{\mathbf{C}}_{PE}^H \right] = \underline{\mathbf{C}}_{PE} \cdot \underline{\mathbf{C}}_{PE}^H. \quad (24)$$

So, computing the IF algorithm comes back to perform the CPEE algorithm for the PN estimation. Therefore, in OFDM systems, we need to use ICI compensation algorithms for compensating the PN effects and then, to enhance the system performance.

## III. DERIVATION OF CROSS-CORRELATION MATRICES AND MSE

The challenge in applying the IF algorithm relies in estimating the cross-correlation matrix of the PN in real scenario. In the case of single carrier and DFT-s-OFDM systems, we will show that it is possible to obtain a theoretical expression based on the knowledge of the PN PSD.

### A. Single Carrier system

Let us denote by  $\mathbf{F}$  and  $\mathbf{S}$  respectively the Fourier transform matrix and the diagonal matrix that contains the sum of the PSD of the PN at the transmitter and receiver on its diagonal. The theoretical expression of the generated discrete-time PN can be expressed as follows [13]:

$$\begin{aligned} \underline{\phi} &= \Re_c \left\{ \sqrt{F_s} \mathbf{F}^H \sqrt{\mathbf{S}} \underline{\mathbf{w}} \right\} \\ &= \sqrt{F_s} \Re_c \left\{ \mathbf{F}^H \sqrt{\mathbf{S}} \underline{\mathbf{w}} \right\} \\ &= \sqrt{F_s} \Re_c \left\{ (\mathbf{F}_R + j\mathbf{F}_I)^H \sqrt{\mathbf{S}} (\underline{\mathbf{w}}_R + j\underline{\mathbf{w}}_I) \right\} \\ &= \sqrt{F_s} \left( \mathbf{F}_R^T \sqrt{\mathbf{S}} \underline{\mathbf{w}}_R - \mathbf{F}_I^T \sqrt{\mathbf{S}} \underline{\mathbf{w}}_I \right) \\ \underline{\phi} &= \sqrt{F_s} \left( \mathbf{F}_R \sqrt{\mathbf{S}} \underline{\mathbf{w}}_R - \mathbf{F}_I \sqrt{\mathbf{S}} \underline{\mathbf{w}}_I \right), \end{aligned} \quad (25)$$

where  $F_s$  is the sampling frequency. The term  $\underline{\mathbf{w}}$  represents an independent and identically distributed complex Gaussian vector of size  $N_p = N_x \cdot N_b$ , where  $N_p$  is the size of the transmitted sequence. It is defined as follows:

$$\underline{\mathbf{w}} \sim \mathcal{CN}(\underline{\mathbf{m}}_{\mathbf{w}}, \mathbf{\Gamma}_{\mathbf{w}}) = \begin{cases} \underline{\mathbf{m}}_{\mathbf{w}} = [0, \dots, 0]^T \\ \mathbf{\Gamma}_{\mathbf{w}} = \mathbf{I}_{N_p}. \end{cases} \quad (26)$$

The vectors  $\underline{\mathbf{w}}_R$  and  $\underline{\mathbf{w}}_I$  in (25) are respectively the real part and the imaginary part of the vector  $\underline{\mathbf{w}}$ . Therefore, the theoretical expression of the cross-correlation matrix of the PN is obtained as follows:

$$\begin{aligned} \mathbf{R}_{\underline{\phi}} &= E \left[ \underline{\phi} \cdot \underline{\phi}^H \right] \\ &= \frac{F_s}{2} \left( \mathbf{F}_R \mathbf{S} \mathbf{F}_R^T + \mathbf{F}_I \mathbf{S} \mathbf{F}_I^T \right), \end{aligned} \quad (27)$$

where  $\mathbf{S}$  is of size  $N_p \times N_p$  and  $\mathbf{R}_{\underline{\phi}}$  is of size  $N_x \times N_x$ . The matrices  $\mathbf{F}_R$  and  $\mathbf{F}_I$  are respectively the real part and the imaginary part of the matrix  $\mathbf{F}$  of size  $N_x \times N_p$ . The elements at the  $i^{\text{th}}$  row and  $k^{\text{th}}$  column of the matrix  $\mathbf{F}$  are obtained as follows:

$$\mathbf{F}^{(i,k)} = \frac{1}{\sqrt{N_p}} e^{-j2\pi \frac{(i-1)(k-1)}{N_p}}, \quad (28)$$

TABLE I  
SIMULATION PARAMETERS

Sampling Frequency	$F_s$	1966.08 MHz
Numerology	$\mu$	4 to 8
Signal bandwidth	$B$	983.04 MHz
Carrier frequency	$F_c$	140 GHz
Phase noise model		3GPP [10]
Tx IFFT size	$N$	$8192 \times 2^{-\mu+4}$
Number of active carriers	$N_s$	$4096 \times 2^{-\mu+4}$
LDPC coding rate	CR	0.3, 0.7 and 0.9
LDPC decoder		Layered Min-Sum
Modulation	$M$	4, 16 and 64 QAM

for  $i = \llbracket 1, \dots, N_x \rrbracket$  and  $k = \llbracket 1, \dots, N_p \rrbracket$ . To express the cross-correlation matrix of the vector  $e^{j\phi}$ , we use the small-angle approximation  $e^{j\phi} \simeq \mathbf{1}_{N_x} + j\phi$  and we obtain:

$$\begin{aligned} \mathbf{R}_{e^{j\phi}} &\simeq E \left[ e^{j\phi} \cdot e^{j\phi H} \right] \\ &\simeq E \left[ (\mathbf{1}_{N_x} + j\phi) (\mathbf{1}_{N_x} + j\phi)^H \right], \quad (29) \\ &\simeq \mathbf{1}_{N_x} + \mathbf{R}_\phi, \end{aligned}$$

with  $\mathbf{R}_\phi$  defined in (27). Considering a single carrier system, the term  $N_x = N_a$ . Furthermore, we derive the theoretical expression of the mean square error (MSE) between the estimated and the generated PN. It is expressed as follows:

$$\begin{aligned} MSE_{HSNR} &= E \left[ \|\mathbf{Z}\mathbf{a}_p^\theta - \phi\|^2 \right], \\ &= \mathcal{T}_r \{ E \left[ (\mathbf{Z}\mathbf{a}_p^\theta - \phi) (\mathbf{Z}\mathbf{a}_p^\theta - \phi)^H \right] \}, \quad (30) \end{aligned}$$

where  $\phi$  is the vector which contains  $\{\phi_i\}_{i \in \mathcal{X}_p}$  values. By replacing (14) in (30), we have:

$$\begin{aligned} MSE_{HSNR} &= \mathcal{T}_r \{ \mathbf{Z}\mathbf{G}_p \mathbf{R}_\phi \mathbf{G}_p^H \mathbf{Z}^H - \mathbf{Z}\mathbf{G}_p \mathbf{R}_\phi \\ &\quad + \mathbf{Z}\mathbf{G}_p \mathbf{R}_n \mathbf{G}_p^H \mathbf{Z}^H \odot \mathbf{s}_p \mathbf{s}_p^H - \mathbf{R}_\phi \mathbf{G}_p^H \mathbf{Z}^H \\ &\quad + \mathbf{R}_\phi \}. \quad (31) \end{aligned}$$

From (31), we can express the MSE between the exponential of the estimated PN and the one of the generated PN as follows:

$$\begin{aligned} MSE &= \mathcal{T}_r \{ \mathbf{Z}\mathbf{G}_p \mathbf{R}_{e^{j\phi}} \mathbf{G}_p^H \mathbf{Z}^H - \mathbf{Z}\mathbf{G}_p \mathbf{R}_{e^{j\phi}} \\ &\quad + \mathbf{Z}\mathbf{G}_p \mathbf{R}_n \mathbf{G}_p^H \mathbf{Z}^H \odot \mathbf{s}_p \mathbf{s}_p^H - \mathbf{R}_{e^{j\phi}} \mathbf{G}_p^H \mathbf{Z}^H \\ &\quad + \mathbf{R}_{e^{j\phi}} \}. \quad (32) \end{aligned}$$

The MSE expression in (31) is obtained assuming the HSNR approximation.

### B. DFT-s-OFDM system

For DFT-s-OFDM system, the exponential vector  $e^{j\phi'}$  can be expressed as follows:

$$e^{j\phi'} = \text{diag} \{ \mathbf{F}_{N_s}^H \mathbf{D} \mathbf{F}_N \mathbf{\Phi}_C \mathbf{F}_N^H \mathbf{M} \mathbf{F}_{N_s} \}, \quad (33)$$

where  $\mathbf{\Phi}_C$  is the diagonal matrix containing the PN shifts  $e^{j\phi}$ .  $\mathbf{F}_X$  is the discrete Fourier transform matrix of size  $X \times X$ . The vector  $\phi$  is the sum of the PN generated by the oscillator at the transmitter and receiver. The matrices  $\mathbf{M}$  and  $\mathbf{D}$  respectively represent the  $N_s$ -to- $N$  mapping matrix and

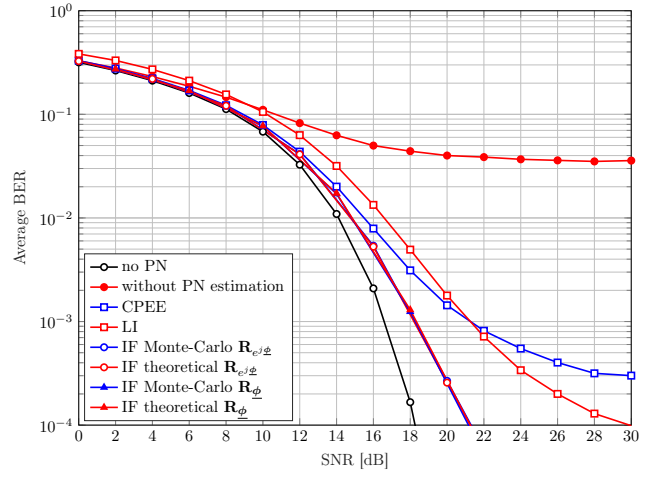


Fig. 1. Uncoded BER performance of a single-carrier system. We use a 16-QAM modulation with the insertion of 16 pilots per block, considering blocks of size  $N_a = 1024$ .

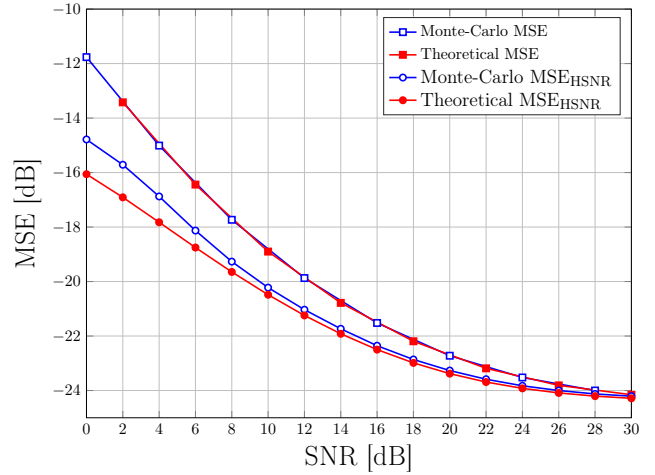


Fig. 2. Theoretical versus Monte-Carlo MSE performance between estimated and generated PN. We consider a 16-QAM modulation with the insertion of 16 pilots per block, considering blocks of size  $N_a = 1024$ .

the  $N$ -to- $N_s$  demapping matrix. By posing  $\mathbf{F}_{RX} = \mathbf{F}_{N_s}^H \mathbf{D} \mathbf{F}_N$  and  $\mathbf{F}_{TX} = \mathbf{F}_N^H \mathbf{M} \mathbf{F}_{N_s}$ , we obtain the relation below:

$$e^{j\phi'} = \mathbf{B} e^{j\phi} \quad \text{with} \quad \mathbf{B}^{(i,k)} = \mathbf{F}_{RX}^{(i,k)} \mathbf{F}_{TX}^{(k,i)} \quad (34)$$

with  $i \in \llbracket 1, \dots, N_s \rrbracket$  and  $k \in \llbracket 1, \dots, N \rrbracket$ . Therefore, the cross-correlation matrix  $\mathbf{R}$  is expressed as follows

$$\mathbf{R} = E \left[ e^{j\phi'} \cdot e^{j\phi'^H} \right] = \mathbf{B} \mathbf{R}_{e^{j\phi}} \mathbf{B}^H. \quad (35)$$

In the case of a DFT-s-OFDM system, the term  $N_x = N$ , where  $N$  represents the size of FFT/IFFT blocks. From (29), the matrix  $\mathbf{R}_{e^{j\phi}}$  is expressed as show in (36):

$$\mathbf{R}_{e^{j\phi}} \simeq \mathbf{1}_N + \mathbf{R}_\phi \quad (36)$$

and consequently, the expression in (35) becomes:

$$\mathbf{R} \simeq \mathbf{B} \left( \mathbf{1}_N + \mathbf{R}_\phi \right) \mathbf{B}^H, \quad (37)$$

with  $\mathbf{R}_\phi$  defined in (27). Then, we can derive the theoretical expression of the MSE between the exponential of the estimated PN and the one after Fourier Transformation as follows:

$$\begin{aligned} MSE = & \mathcal{T}_r \{ \mathbf{Z} \mathbf{G}_p \mathbf{R}_{e^{j\phi'}} \mathbf{G}_p^H \mathbf{Z}^H - \mathbf{Z} \mathbf{G}_p \mathbf{R}_{e^{j\phi}} \\ & + \mathbf{Z} \mathbf{G}_p \mathbf{R}_n \mathbf{G}_p^H \mathbf{Z}^H \odot \mathbf{s}_p \mathbf{s}_p^H - \mathbf{R}_{e^{j\phi'}} \mathbf{G}_p^H \mathbf{Z}^H \\ & + \mathbf{R}_{e^{j\phi}} \}. \end{aligned} \quad (38)$$

#### IV. NUMERICAL RESULTS

In this section, we present system performance based on the parameters summarized in the TABLE I. The signal-to-noise ratio (SNR) is evaluated overall the bandwidth. For the PN estimation, we consider phase tracking reference signal (PTRS) distribution as depicted in Fig. 1-(a) in [7]. We consider a realistic channel estimation with noisy received pilots.

##### A. Theoretical vs Monte-Carlo Analysis

Fig. 1 presents the system performance of a single-carrier system in terms of uncoded BER. IF, CPEE and LI algorithms are considered for PN estimation. Regarding the IF algorithm, we consider: (i) first, the theoretical cross-correlation matrix  $\mathbf{R}_{e^{j\phi}}$  as expressed in (29), and the one obtained by Monte-Carlo simulations, (ii) second, the theoretical cross-correlation matrix  $\mathbf{R}_\phi$  expressed in (27) and the one obtained by Monte-Carlo simulations. We transmit a frame of  $N_p = 65536$  samples. Before the symbols detection, we operate the PN estimation and compensation on blocks of 1024 samples.

Regarding the IF algorithm, we observe that the system performance obtained by using theoretical cross-correlation matrices in Sec. III-B match well with those obtained with the Monte-Carlo one.

Fig. 2 presents the comparison between the theoretical and the Monte-Carlo MSE. We consider the theoretical MSE expressions in (31) and (32). We show once again a good match between theoretical MSE expressed in (32) and the Monte-Carlo. For the MSE expression in (31), a performance gap is observed in low SNR: the HSNR approximation is no longer valid.

##### B. Coded TBLER Performance

For 5G-NR multicarrier waveforms, we perform coded TBLER simulations. A 5G-NR low density parity check (LDPC) code [14] and extended numerologies [8] are considered. For OFDM systems, we consider a fast Fourier transform (FFT) block of size  $N$ . For DFT-s-OFDM systems, the DFT spreading block of size  $N_s$  is appended to the OFDM FFT. The OFDM and DFT-s-OFDM systems are compared for same signal bandwidth, *i.e.* only  $N_s$  subcarriers over  $N$  are actives in OFDM. When it comes to the PN estimation, three algorithms are investigated: (i) CPEE, (ii) LI and (iii) the proposed IF. The achieved performance of OFDM are depicted in TABLE II and those of DFT-s-OFDM in TABLE III, where we also represent the spectral efficiency (SE). The SE is defined by the product

$$SE = \log_2(M) \cdot CR, \quad (39)$$

where  $M$  and CR are respectively the modulation order and the LDPC coding rate. We consider three levels: (i) low SE

considering a QPSK modulation with CR= 0.3. (ii) Medium SE for a 16-QAM modulation with CR= 0.7 and (iii) high SE for a 64-QAM modulation with CR= 0.9.

The performance metric considered for the performance evaluation is the SNR value to ensure a given TBLER target at  $10^{-2}$ . NA stands for "not achievable". Regarding to the IF algorithm, we consider:

- first, a perfect knowledge of cross-correlation matrices  $\mathbf{R}$ ,  $\mathbf{R}_I$  and  $\mathbf{R}_n$  (20) by estimating them from training sequences. The results are mentioned in the column "IF simu." of TABLES II and III.
- second, we consider the first case but, we replace the matrix  $\mathbf{R}$  in (21) by the theoretical cross-correlation matrix of the exponential of the PN generated by the oscillators in (37). In addition, we also neglect the cross-correlation matrix of the ICI, *i.e.*  $\mathbf{R}_I$ , because it could be difficult to estimate this matrix correctly in real scenario. The results are presented in the column "IF theo." of TABLE III.

For OFDM systems, as represented in TABLE II and mentioned in Sec. II-C, doing the IF algorithm is equivalent to doing the CPEE algorithm. For  $\mu \geq 4$ , the CPEE algorithm is sufficient for PN estimation in low SE. In medium SE, the CPEE algorithm can be implemented for  $\mu \geq 6$ . Indeed, the more we increase the numerology, the more we reduce the ICI by increasing the subcarrier spacing (SCS). For  $\mu < 6$ , ICI compensation algorithms as presented in [4] might be needed to improve the system performance. In high SE, the CPEE algorithm only reaches the target TBLER for  $\mu = 8$ . Therefore, ICI cancellation techniques are needed in high SE.

Regarding DFT-s-OFDM system performance in TABLE III, CPEE provides the same performance as IF in low SE. LI is the worst performing algorithm to implement compared to CPEE and IF algorithms. In medium SE, we observe that for  $\mu > 6$ , CPEE and IF provide the same performance, and LI algorithm is less better than CPEE. In contrast, for  $\mu \leq 6$ , the SNR gain by using IF instead of CPEE increases (SNR > 2 dB). This is because of the increasing of the SE. Also, considering low numerologies means big size of DFT and FFT blocks and therefore, a bad estimation using CPEE. LI algorithm is better than CPEE but less than IF. In high SE, we observe that CPEE is the least efficient algorithm to use. We observe a SNR gain of 1.2 dB in average by using the IF algorithm instead of LI. Finally, according to IF algorithm, both IF simu. and IF theo. provide similar system performance.

##### C. Discussion

First of all, one can observe that the simulation results match well with the theoretical expressions (Fig. 1) for single-carrier systems. When it comes to multicarrier waveforms, one can observe that ICI cancellation techniques are required in OFDM systems for high SE. For DFT-s-OFDM systems, one can observe that the simulation performance match the expected theoretical results. It validates the implementation of IF algorithm in DFT-s-OFDM system with theoretical expression of the PN correlation matrix in (29). According to the numerical results and simulation parameters used, the

TABLE II  
EVALUATION OF SNR [DB] VALUES TO MEET TBLER TARGET  $10^{-2}$  FOR OFDM SYSTEMS ASSUMING A PILOT DENSITY OF 12.5%.

		(M - CR)	(QPSK - 0.3)			(16-QAM - 0.7)			(64-QAM - 0.9)		
		SE	0.6			2.8			5.4		
		Algorithms	CPEE	LI	IF simu.	CPEE	LI	IF simu.	CPEE	LI	IF simu.
$\mu$	4	240 kHz	-3.83	-0.66	-3.84	NA	NA	NA	NA	NA	NA
	5	480 kHz	-4.02	-0.89	-4.02	22.19	NA	22.59	NA	NA	NA
	6	960 kHz	-4.05	-1.03	-4.05	9.04	11.42	9.05	NA	NA	NA
	7	1920 kHz	-4.05	-1.04	-4.05	7.57	9.18	7.57	NA	NA	NA
	8	3840 kHz	-4.02	-1.02	-4.02	7.33	8.89	7.34	21.40	31.79	21.33

TABLE III  
EVALUATION OF SNR [DB] VALUES TO MEET TBLER TARGET  $10^{-2}$  FOR DFT-S-OFDM SYSTEMS ASSUMING A PILOT DENSITY OF 12.5%.

		(M - CR)	(QPSK - 0.3)				(16-QAM - 0.7)				(64-QAM - 0.9)			
		SE	0.6				2.8				5.4			
		Algorithms	CPEE	LI	IF simu.	IF theo.	CPEE	LI	IF simu.	IF theo.	CPEE	LI	IF simu.	IF theo.
$\mu$	4	240 kHz	-3.83	-1.21	-4.16	-4.16	NA	8.57	7.19	7.19	NA	18.36	16.99	16.98
	5	480 kHz	-4.02	-1.21	-4.15	-4.12	NA	8.58	7.19	7.19	NA	18.38	16.98	16.98
	6	960 kHz	-4.05	-1.21	-4.10	-4.09	9.12	8.58	7.19	7.19	NA	18.40	16.98	16.98
	7	1920 kHz	-4.05	-1.12	-4.06	-4.06	7.57	8.59	7.19	7.19	NA	18.52	16.98	16.98
	8	3840 kHz	-4.02	-1.04	-4.02	-4.02	7.33	8.73	7.19	7.19	22.00	18.69	17.00	16.99

ICI contribution can be neglected for DFT-s-OFDM systems. This simplifies the model and thus the implementation of the IF compensation technique, assuming the pilot density used in this work. However, performance degradation could possibly appear if one increases the PN power (by increasing the carrier frequency) or the modulation order. Additionally, it seems important not to forget that this simplification depends on the correlated nature of the PN and may not always be valid (for example if one consider uncorrelated phase noise as presented in [15]). As a reminder, all the presented results are obtained by assuming a perfect knowledge of the PN PSD, and considering the LoS channel model as defined in Sec. II-A.

## V. CONCLUSION

Ensuring proper PN estimation and compensation in sub-THz transmissions is critical. In this work, we extended the work done in [7] about a solution called interpolation filter (IF). The proposed algorithm is based on the use of correlation information of the PN to track it. We performed numerical simulations considering single-carrier, OFDM and DFT-s-OFDM systems. The presented results are validated by theoretical expressions, by assuming the knowledge of the PN PSD. For OFDM systems, the IF algorithm provides the same performance as the CPEE algorithm. As a consequence, considering the proposed IF technique for OFDM is not interesting as CPEE is easier to implement. ICI cancellation algorithms might be needed for increasing the SE. When it comes to single-carrier and DFT-s-OFDM systems, we presented the same system performance considering the IF algorithm, by using the theoretical PN cross-correlation matrix expressed in Sec. III-B and the one obtained with Monte-Carlo simulations. These results validated the theoretical expressions of the PN cross-correlation matrix derived in this work, and the possibility of implementing the IF algorithm in real scenario.

## REFERENCES

- [1] J.-B. Doré, Y. Corre, S. Bicaïs, J. Palicot, E. Faussurier, D. Kténas, and F. Bader, "Above-90GHz Spectrum and Single-Carrier Waveform as Enablers for Efficient Tbit/s Wireless Communications," in *Proc. Int. Conf. Telecommunications (ICT)*, Saint-Malo, France, Jun 2018.
- [2] V. Petrov, T. Kurner, and I. Hosako, "IEEE 802.15.3d: First Standardization Efforts for Sub-Terahertz Band Communications toward 6G," *IEEE Commun. Mag.*, 2020.
- [3] D. Petrovic, W. Rave, and G. Fettweis, "Intercarrier interference due to phase noise in OFDM - estimation and suppression," in *Proc. IEEE Veh. Technol. Conf. (VTC-Fall)*, 2004.
- [4] M. Afshang, D. Hui, J.-F. T. Cheng, and S. Grant, "On Phase Noise Compensation for OFDM Operation in 5G and Beyond," in *Proc. IEEE Wireless Commun. and Netw. Conf. (WCNC)*, 2022.
- [5] J.-C. Sibel, "Pilot-Based Phase Noise Tracking for Uplink DFT-s-OFDM in 5G," in *Proc. Int. Conf. Telecommunications (ICT)*, 2018.
- [6] M. Chung, L. Liu, and O. Edfors, "Phase-Noise Compensation for OFDM Systems Exploiting Coherence Bandwidth: Modeling, Algorithms, and Analysis," *IEEE Trans. on Wireless Commun.*, vol. 21, 2022.
- [7] Y. Bello, J.-B. Doré, and D. Demmer, "DFT-s-OFDM for sub-THz Transmission - Tracking and Compensation of Phase Noise," in *Proc. IEEE Consum. Commun. & Netw. Conf. (CCNC)*, 2023.
- [8] O. Tervo, I. Nousiainen, I. P. Nasarre, E. Tirola, and J. Hukkukonen, "On the Potential of Using Sub-THz Frequencies for Beyond 5G," in *Proc. Joint European Conf. on Netw. and Commun. & 6G Summit (EuCNC/6G Summit)*, 2022.
- [9] L. Pomietcu and R. D'Errico, "An Indoor Channel Model for High Data-Rate Communications in D-Band," *IEEE Access*, vol. 8, 2020.
- [10] 3GPP, "Study on new radio access technology: Radio Frequency (RF) and co-existence aspects," TS 38.803, 2017-09.
- [11] R. Krishnan, M. R. Khanzadi, T. Eriksson, and T. Svensson, "Soft Metrics and Their Performance Analysis for Optimal Data Detection in the Presence of Strong Oscillator Phase Noise," *IEEE Trans. on Commun.*, 2013.
- [12] Yingshan Li, Heung-Gyoon Ryu, Li-jie Zhou, Dongyan Sun, Haiyuan Liu, and Junwen Li, "Frequency offset and phase noise influence and its compensation in the DFT-spread OFDM system," in *Proc. Int. Conf. on Commun., Circuits and Syst. (ICCCAS)*, 2008.
- [13] 3GPP, "RF Impairment models for 60GHz-band SYS/PHY Simulation," Project IEEE 802.15-06-0477-00-003c, November, 2006.
- [14] —, "Overall Description Stage 2," TS 38.300, 2017-12.
- [15] S. Bicaïs and J.-B. Doré, "Phase Noise Model Selection for Sub-THz Communications," in *Proc. IEEE Global Commun. Conf. (GLOBECOM)*, 2019.